Acta Crystallographica Section A
Foundations of Crystallography
ISSN 0108-7673

Received 18 April 2003
Accepted 13 May 2003

Improving triplet-phase accuracy by symmetry observations in reference-beam diffraction measurements

Qun Shen

Cornell High Energy Synchrotron Source (CHESS) and Department of Materials Science and Engineering, Wilson Laboratory, Cornell University, Ithaca, NY 14853, USA. Correspondence e-mail: qs11@cornell.edu

The reference-beam X-ray diffraction technique allows parallel measurements of many three-beam interference profiles in a modified rotating-crystal experiment. Because of the unique symmetry relations that exist in the reference-beam geometry, a complete 360° rotation leads to a *four*fold redundancy of any given triplet phase δ_H involving primary reflection **H**, reference reflection **G** and coupling reflection **H**−**G**, measured in a data set. Two such redundant measurements correspond to simple duplications with the reciprocal node **H** going into and coming out of the Ewald sphere, while the other two correspond to the Friedel mate **G**−**H** of the coupling reflection **H**−**G** passing through the Ewald sphere in a similar fashion. It is shown that substantial differences may exist between the **H** and the **G**−**H** cases, with an enhanced triplet-phase interference effect in one of them. These symmetry-related observations, coupled with inverse-beam triplet measurements, would improve the phase measurement accuracy of the reference-beam diffraction technique.

1. Introduction

Direct measurements of triplet phases by three-beam diffraction have been demonstrated on protein crystals in the past decade (Chang *et al.*, 1991; Weckert *et al.*, 1993; Weckert & Hümmer, 1997; Weckert *et al.*, 1999; Shen, 1999*a*; Chang *et al.*, 1999; Mo *et al.*, 2002; Shen & Wang, 2003). In a traditional three-beam diffraction experiment, the intensity I_H for a primary reflection **H** is monitored while an azimuthal rotation ψ is applied to bring another reciprocal node **G** through the Ewald sphere (see *e.g.* Weckert & Hümmer, 1997). In a recently developed reference-beam diffraction (RBD) technique (Shen, 1998), intensities I_H of many primary reflections **H** are simultaneously recorded on an area detector by the rotating-crystal method while stepping rocking angle θ through a secondary reflection **G**. The reference-beam diffraction technique allows substantial improvements in three-beam measurement time needed for protein crystals (Shen, 1999*a*; Chang *et al.*, 1999; Shen *et al.*, 2000*a*,*b*, 2002; Pringle & Shen, 2003) and in systematic phasing of individual structure factors from a measured triplet data set (Shen & Wang, 2003). These improvements make three-beam phasing more practical in a data-collection environment familiar to protein crystallographers.

One of the important issues in all three-beam experiments is the accuracy of the measured triplet phases from three-beam interference profiles of intensity I_H *versus* azimuthal angle ψ in the conventional azimuthal scan method, or I_H *versus* rocking angle θ in the reference-beam geometry. In the conventional method, since each interference profile is measured one at a time using a point detector, it is straightforward to achieve certain intensity measurement accuracy by applying a proper counting time for each triplet combination. In the reference-beam method, however, all primary reflections recorded on an oscillation image are measured in parallel with the same exposure time on the area detector, causing considerable variation in measurement accuracy between strong and weak reflections. Thus, how to improve measured triplet phase accuracy remains under research investigation in the reference-beam diffraction geometry.

Several methods can be used to increase the measurement accuracy in reference-beam diffraction. Firstly, an area detector with a larger dynamic range can be used to record the reference-beam diffraction images. Secondly, the same oscillation diffraction image can be measured twice with two different exposure times, one suitable for strong reflections and the other for weak reflections. Finally, additional symmetry relations in reference-beam geometry can be exploited to increase the data redundancy by multiple measurements of the same triplet phase. These symmetry relations are completely general and space-group independent, since they are in addition to all the symmetry operations given by any space group.

In this paper, we examine three additional symmetry elements that are unique in reference-beam diffraction. The first is the in/out symmetry of a given primary reflection **H**, with **G** as the reference beam. This leads to completely redundant measurements of triplet phase δ_H for three-beam combination **H**/**G**/**H**−**G**. The second is a reference-beam modified Friedel symmetry that provides a measurement of the same triplet phase δ_H with the same reference reflection **G** but on the inverse-coupling reflection **G**−**H**/**G**/−**H**. The third is the triplet inversion symmetry with inverse reference beam −**G** that gives rise to the measurement of δ_{-H} for triplet −**H**/−**G**/**G**−**H**. We show that indeed not only can redundant measurements increase the triplet-phase precision but certain symmetry-related observations, such as **G**−**H**/**G**/−**H**, may be more advantageous than others, and lead to more pronounced three-beam interference profiles for the same triplet phase.

2. Symmetry elements

In a reference-beam diffraction process **H**/**G**/**H**−**G**, with **G** as the reference, **H** as the primary and **H**−**G** as the coupling reflections, reflection **H** passes through the Ewald sphere at rotation angle ψ given by (Shen *et al.*, 2000*b*)

$$\cos\psi = \frac{\sin\theta_H - \cos\beta\sin\theta_G}{\sin\beta\cos\theta_G}, \qquad (1)$$

where β is the angle between the **H** and the **G** reciprocal vectors, θ_H is the Bragg angle for **H**, θ_G for **G** and ψ is defined as the angle between the scattering plane formed by **G** and incident wavevector **k** and that formed by **G** and **H**. Equation (1) is essentially the same as that for conventional three-beam diffraction. When θ_G equals zero, equation (1) reduces to the condition for the conventional oscillation method.

Using Bragg conditions for **H** and **G**, it is straightforward to solve for wavelength λ as a function of rotation angle ψ:

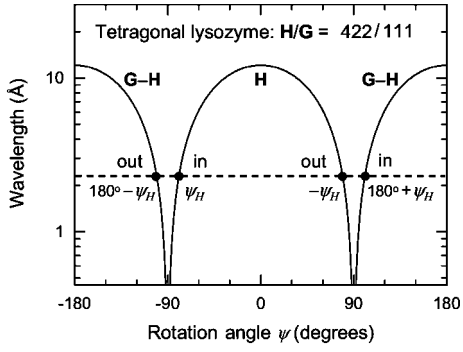

Figure 1
Illustration of rotation-angle positions ψ at which a primary reflection **H** passes through the Ewald sphere in reference-beam diffraction geometry, with reference reflection **G** as the detour reflection. The example given is for **H** = 422 and **G** = 111 in tetragonal lysozyme. The four ψ positions at a given wavelength correspond to **H** and its coupling Friedel mate **G**−**H** going *in* to and coming *out* of the Ewald sphere, respectively. All four cases lead to three-beam effects with the same detour reflection **G** and same triplet phase δ_H. However, different interference amplitudes may exist between the **H** and the **G**−**H** cases owing to the relative strengths of the structure factors.

$$\lambda = \frac{2d_G\sin\beta|\cos\psi|}{[(d_G/d_H - \cos\beta)^2 + \sin^2\beta\cos^2\psi]^{1/2}}. \qquad (2)$$

Fig. 1 shows an example of λ *versus* ψ dependence in a 360° rotation for a given primary reflection **H** = 422 and reference reflection **G** = 111 for a tetragonal lysozyme crystal (space group $P4_32_12$, unit cell $a = b = 78.5$, $c = 37.8$ Å). Obviously, every primary reflection **H** has a different but similar curve, with its own rotation-angle zero setting $\psi = 0$ defined when reciprocal vector **H** is within the **G** scattering plane as shown in Fig. 2(*a*).

Equations (1) and (2) define the symmetry properties in reference-beam diffraction geometry for any given primary reflection **H**. These symmetry elements are in addition to the Laue symmetry operations given by the space group of the crystal structure. We now go through these additional elements in more detail.

2.1. In–out symmetry

As shown in Fig. 1, at a given wavelength $\lambda = \lambda_0$, there are four occurrences for a primary reflection **H**, corresponding to the four interception points of $\lambda = \lambda_0$ with the $\lambda(\psi)$ curve. Two such cases, related by $\pm\psi$, are due to the fact that cos ψ is an even function and the solution $\pm\psi$ corresponds to the same reciprocal node **H** passing through the Ewald sphere from outside to inside and then from inside to outside situations. These in–out conditions have been considered in the context of a conventional ψ-scan three-beam method (Chang, 1982), where a sign change takes place in three-beam interference profiles between the 'in' and the 'out' cases.

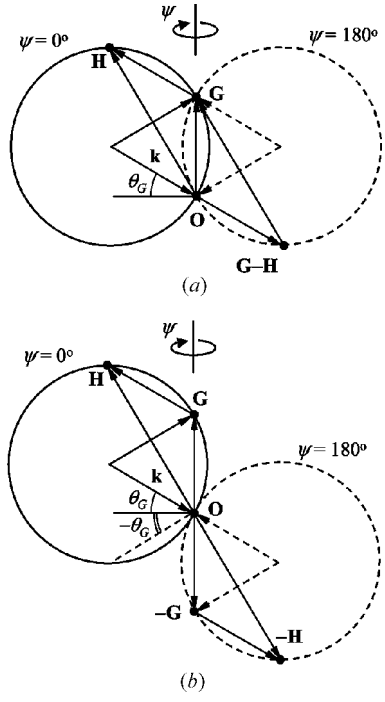

Figure 2
Schematics of geometric relations between (*a*) the **H**/**G**/**H**−**G** case and its coupling Friedel mate **G**−**H**/**G**/−**H**, and (*b*) the **H**/**G**/**H**−**G** case and its complete triplet inversion −**H**/−**G**/**G**−**H**.

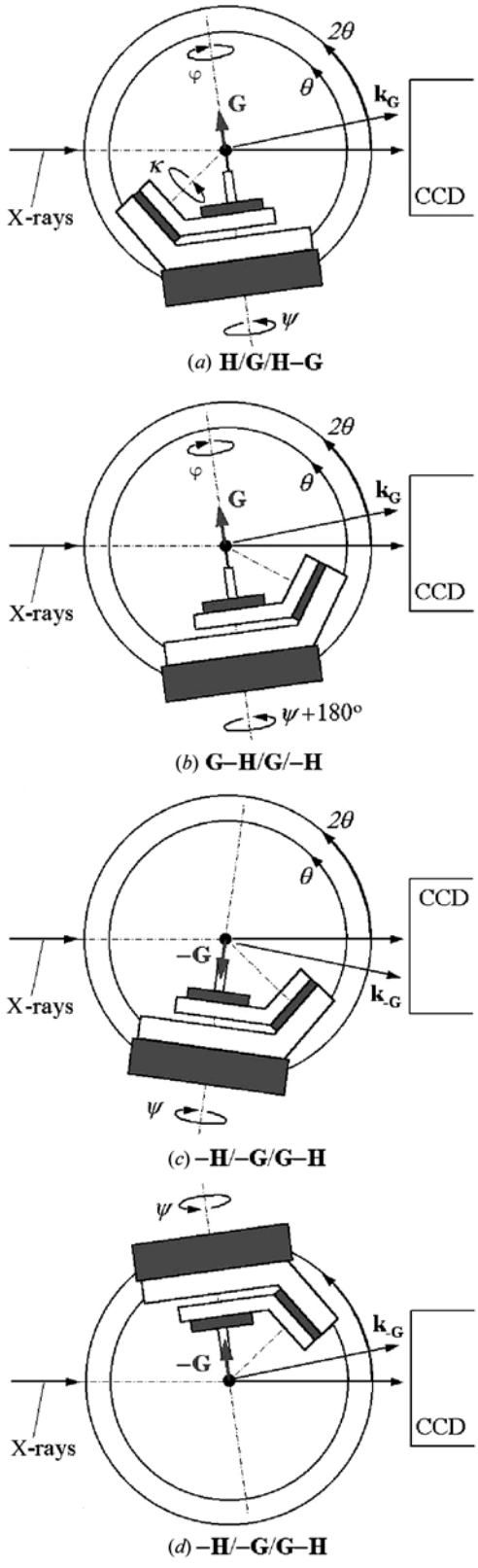

Figure 3
Illustrations of symmetry-related reference-beam diffraction measurements using a special κ diffractometer (Pringle & Shen, 2003): (*a*) primary reflection **H**/**G**/**H**−**G** at rotation angle ψ and rocking angle θ; (*b*) Friedel mate of the coupling reflection **G**−**H**/**G**/−**H** at ψ+180° and θ; (*c*) inverse-beam triplet −**H**/−**G**/**G**−**H** at ψ+180° and $-\theta$; and (*d*) inverse-beam case −**H**/−**G**/**G**−**H** at ψ and θ+180°.

In reference-beam diffraction geometry, however, since the **H** reflection is the primary reflection and the reference **G** reflection is actually the detour excitation, the interference profiles measured in these in/out cases for **H**/**G**/**H**−**G** are completely identical as long as the same rocking angle θ_G direction is employed, which is usually the case. Thus, measurements at $\pm\psi$ provide a redundancy of two for any given **H**/**G**/**H**−**G** triplet with triplet phase $\delta_H = \alpha_G + \alpha_{H-G} - \alpha_H$, where the α_H's are the individual structure-factor phases.

2.2. Coupling inversion symmetry

Fig. 1 illustrates that the $\lambda(\psi)$ curve for each **H** reflection consists of two branches: one centred at $\psi = 0$ and the other at $\psi = 180°$, as derived from equation (2). However, as shown in Fig. 2(*a*), the branch at $\psi = 180°$ is in fact due to the Friedel mate **G**−**H** of the coupling reflection **H**−**G**, which we will term as the *inverse coupling reflection*. The best way to rigorously derive this additional symmetry is to use the vector form of the Bragg condition for primary reflection **H**:

$$|\mathbf{H} + \mathbf{k}| = k,$$

where **k** is the incident wavevector ($k = |\mathbf{k}|$), with its component $\mathrm{k}_\parallel$ parallel to **G** given by the Bragg law for reference reflection **G**:

$$k_\parallel = -G/2.$$

With the above two equations, it is easy to obtain the following diffraction condition for **H** with **G** reflection excited:

$$2\mathbf{H}_\perp \cdot \mathbf{k}_\perp = H_\parallel G - H^2, \qquad (3)$$

where $G = |\mathbf{G}|$, $H = |\mathbf{H}|$ and $\perp$ and $\parallel$ denote the vector components perpendicular and parallel to **G**, respectively. Now if reflection **M** = **G**−**H** is considered, it is obvious that

$$\mathbf{M}_\perp = -\mathbf{H}_\perp, \quad M_\parallel = G - H_\parallel,$$

and therefore

$$\mathbf{M}_\perp \cdot \mathbf{k}_\perp = \mathbf{H}_\perp \cdot (-\mathbf{k}_\perp), \qquad (4)$$

which means that reciprocal node **G**−**H** always passes through the Ewald sphere exactly at $\Delta\psi = 180°$ from where **H** passes through.

We should note that when **G** = 0 we recover the situation in the standard rotating-crystal method where the measurement at $\Delta\psi = 180°$ corresponds to that for the Friedel mate −**H**. In our present reference-beam situation, if the triplet interference profile for **H**/**G**/**H**−**G** is recorded at ψ_H, then the interference profile for its coupling Friedel mate, **G**−**H**/**G**/−**H**, will always appear at $\psi_{G-H} = \psi_H + 180°$. The triplet phase δ_{G-H} in this case is equal to $\delta_{G-H} = \alpha_G + \alpha_{-H} - \alpha_{G-H}$, which is identical to $\delta_H = \alpha_G - \alpha_H + \alpha_{H-G}$ if anomalous dispersion is negligible. However, since the magnitude of structure factor $|F_{G-H}|$ is not necessarily equal to $|F_H|$, the interference profile for **G**−**H**/**G**/−**H** can be very different from that for **H**/**G**/**H**−**G**. We will illustrate this point in §4 through an example.

Table 1
Symmetry-related observations in reference-beam diffraction using a κ diffractometer.

Symmetry element	In–out	Coupling inversion	Triplet inversion	Coupling triplet inversion
Triplet reflection	**H/G/H−G**	**G−H/G/−H**	**−H/−G/G−H**	**H−G/−G/H**
Primary reflection	**H**	**G−H**	**−H**	**H−G**
Detour reflection	**G**	**G**	**−G**	**−G**
Triplet phase	δ_H	δ_H	$-\delta_H$	$-\delta_H$
Alignment setting	κ, φ	κ, φ	κ, φ	κ, φ
Rotation angle ψ	$\pm\psi_H$	$\pm\psi_H$+180°	$\pm\psi_H$+180°	$\pm\psi_H$
Rocking angle θ	θ_G	θ_G	$-\theta_G$	$-\theta_G$

2.3. Triplet inversion symmetry

Triplet inversion symmetry refers to the inversion of every reciprocal vector in a three-beam combination **H/G/H−G** to its Friedel mate, **−H/−G/G−H**, as illustrated in Fig. 2(*b*). In this case, the triplet phase measured in the interference profile is $\delta_{-H} = \alpha_{-G} + \alpha_{G-H} - \alpha_{-H} = -\delta_H$, assuming again that anomalous dispersions are negligible in the structure factors. The same symmetry transforms the inverse-coupling reflection case **G−H/G/−H** into **H−G/−G/H**, which has the same triplet phase $-\delta_H$.

The inverse-triplet measurements, in general, are useful for two reasons. Firstly, these measurements allow an unambiguous determination of the enantiomorph for noncentrosymmetric systems (Weckert & Hümmer, 1997; Chang *et al.*, 1999; Shen *et al.*, 2000*a*). Secondly, by comparing a pair of three-beam interference profiles related by inversion symmetry, a more accurate triplet phase value can be obtained because a phase-independent intensity contribution to the profiles for a mosaic crystal can be separated out by the measurement (Weckert *et al.*, 1993; Weckert & Hümmer, 1997; Chang *et al.*, 1999; Shen & Wang, 2003).

3. Experimental set-up

While the symmetry-related three-beam cases mentioned above can be measured in the conventional ψ-scan technique, the reference-beam diffraction method is particularly useful in providing a simple and systematic approach for all three types of symmetry-related measurements. The use of oscillation data collection in reference-beam diffraction also allows applications of many methodologies that already exist in standard oscillation experiments with only slight modifications.

In order to perform systematic symmetry observations in a reference-beam diffraction experiment, we have recently installed a compact five-circle κ diffractometer at CHESS and used it for reference reflection alignment and oscillation data collection (Pringle & Shen, 2003). The κ diffractometer consists of four rotations (κ, φ, ψ, θ) for sample manipulations plus a 2θ arm for a pin-diode detector. The CCD area detector is usually mounted on the base table and not moved during data collection.

In Fig. 3, we show the typical arrangements for measuring the symmetry-related three-beam cases discussed in the last section, with angle settings of the κ diffractometer listed in Table 1. Once the **G** reflection is aligned parallel to the rotation axis ψ by proper (κ, φ) rotations, all eight symmetry observations listed in Table 1, including inverse reference-beam **G** measurements, can be performed easily with appropriate rotation-angle ψ and rocking-angle θ settings in reference-beam data collection.

We should note that the same inverse-triplet condition **−H/−G/G−H** can be reached by keeping the same rotation angle ψ_H and rotating θ by 180° to θ_G + 180°. This, however, would have the disadvantage that the θ drive would position everything upside-down as shown in Fig. 3(*d*), which could mechanically interfere with some equipment mounted around the specimen.

4. Results and discussion

In order to examine how different symmetry reflections affect the reference-beam interference profiles, we have performed theoretical calculations on a tetragonal lysozyme crystal using a distorted-wave diffraction theory developed by our group (Shen, 1999*b*, 2000; Shen & Huang, 2001). Based on this theory, the diffracted intensity I_H for a given primary reflection **H** recorded on a reference-beam oscillation image, normalized to its two-beam intensity, is given by the following analytical expression (Shen, 2000; Shen & Huang, 2001):

$$I_H(\theta) = 1 - p \sin\delta_H \left(\frac{\sin\Delta\theta}{\Delta\theta}\right)^2 + \frac{p}{\Delta\theta}\left(\cos\delta_H + \frac{p}{2\Delta\theta}\right)\left(1 - \frac{\sin(2\Delta\theta)}{2\Delta\theta}\right), \quad (5)$$

where $\Delta\theta = \pi(\theta - \theta_G)t/d_G$, t is the average crystal domain size, d_G is the d spacing of the **G** reflection, p is the interference amplitude and δ_H is the triplet phase of the three-beam combination **H/G/H−G**. For a symmetric **G** reflection, p is given by

$$p = \frac{r_e \lambda t}{V_c \cos\theta_G}\left|\frac{F_G F_{H-G}}{F_H}\right|, \quad (6)$$

where $r_e = 2.82 \times 10^{-5}$ Å is the classical radius of an electron, V_c is the unit-cell volume and F_H is the structure-factor amplitude for reflection **H**. It has been shown that the distorted-wave theory equation (5) is much improved over the second-order Born approximation (Shen, 1986), and is in almost perfect agreement with the full n-beam dynamical theory (Colella, 1974) for macromolecular crystals because the typical crystal size of $t < 0.5$ mm is much smaller than the *Pendellösung* period or the extinction length for these light-element crystals (Shen & Huang, 2001).

In Fig. 4, we show the calculated reference-beam interference profiles using equation (5) for tetragonal lysozyme with primary reflection **H** = $3\bar{1}1$ and reference reflection **G** =

111 at an X-ray wavelength of λ = 1.1 Å. All four cases indicated in Fig. 1 are presented, with 'in' and ''out' situations for both **H** and **G**−**H**, along with the corresponding inverse-beam cases. From Fig. 4, we can derive the following conclusions.

Firstly, the in–out symmetry-related observations for the same primary reflection, **H** or **G**−**H**, are completely identical. As explained in §2, this is because reference **G** serves the role of a detour excitation and **H** is the actual primary reflection. In addition, the same rotation direction for rocking angle θ is usually applied. Thus, there is no sign reversal in reference-beam diffraction geometry as compared to the case of conventional three-beam observations.

Secondly, the **H** and the **G**−**H** profiles, located 180° apart in rotation angle ψ, can be very different in interference strength even though the triplet phase δ_H involved is the same. This is entirely due to the structure-factor amplitude ratios $|F_G F_{H-G}/F_H|$ for these reflections, as indicated by equation (6), and may be used in experiments to select a more pronounced interference profile for measurement of the same δ_H. In the example given in Fig. 4, the **H** reflection is the preferred measurement of δ_H rather than its coupling Friedel mate **G**−**H** reflection.

Thirdly, as already pointed out for conventional three-beam cases (Weckert & Hümmer, 1997), simultaneous measurements of the inverse-beam pair, **H**/**G**/**H**−**G**, and its triplet inversion, −**H**/−**G**/**G**−**H**, can be very helpful in reducing the triplet phase errors due to the phase-independent intensity contributions in a mosaic crystal.

An example of the inverse-beam pair is given in Fig. 5, where we show the measured reference-beam interference profiles for the $3\bar{1}1/111$ and its inverse-beam triplet $\bar{3}1\bar{1}/\bar{1}\bar{1}\bar{1}$ on a tetragonal lysozyme crystal at wavelength λ = 1.097 Å. The data are analyzed by a curve-fitting procedure using equation (5) as discussed in Shen & Wang (2003). The fit results are listed in Fig. 5 and shown as the solid curves. If no inverse-beam case −**H**/−**G**/**G**−**H** were measured, the deduced triplet phase from the $3\bar{1}1/111$ profile alone would be 75°, which deviates considerably from the calculated phase δ_{cal} = 133°. With the inverse-beam $\bar{3}1\bar{1}/\bar{1}\bar{1}\bar{1}$ profile available, a more reliable triplet-phase fit result δ is chosen based on the *larger* of the interference amplitudes p between the two profiles, and the triplet phase of the other case is assigned to the negative of the chosen δ (Shen & Wang, 2003). This '*larger-interference-amplitude*' procedure leads to δ = 132° for the $3\bar{1}1/111$ case,

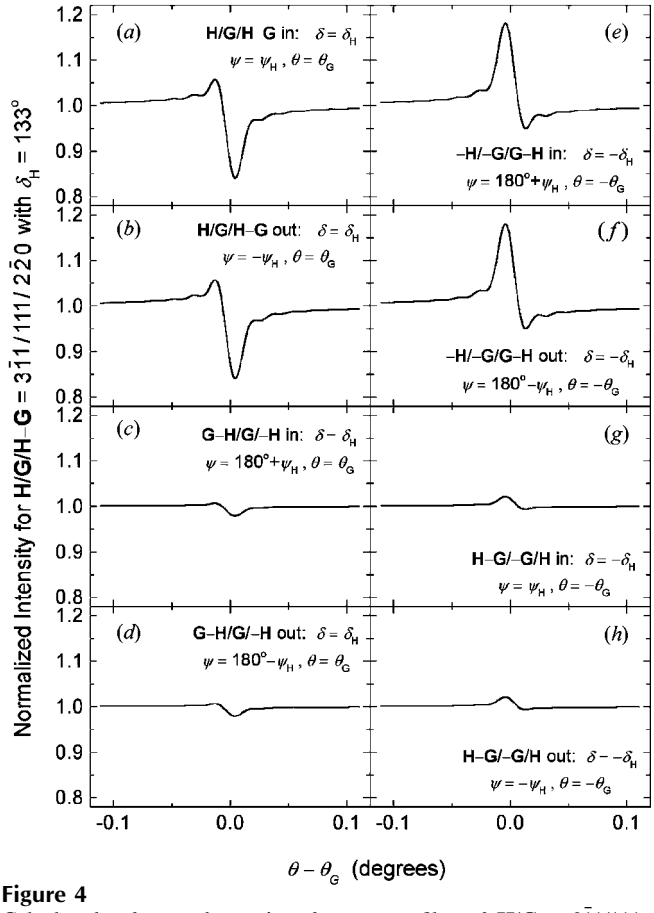

Figure 4
Calculated reference-beam interference profiles of **H**/**G** = $3\bar{1}1/111$ of tetragonal lysozyme, using equation (5), for the four redundant measurements of δ_H on **H** and **G**−**H** (*a*)–(*d*), and their corresponding inverse-beam cases of $-\delta_H$ (*e*)–(*h*). Parameters used in the calculation are: average crystal domain size t = 10 µm, X-ray wavelength λ = 1.1 Å, structure factors $F_G = F_{111}$ = 5004, $F_H = F_{3\bar{1}1}$ = 1589, $F_{H-G} = F_{2\bar{2}0}$ = 4527, and triplet phase δ_H = 133°, based on Vaney *et al.* (1995, 1996). The results indicate that, owing to different reflection strengths, certain interference profiles (*e.g.* on **H** and −**H** in this case) may be more advantageous than others (*e.g.* on **G**−**H** and **H**−**G** in this case).

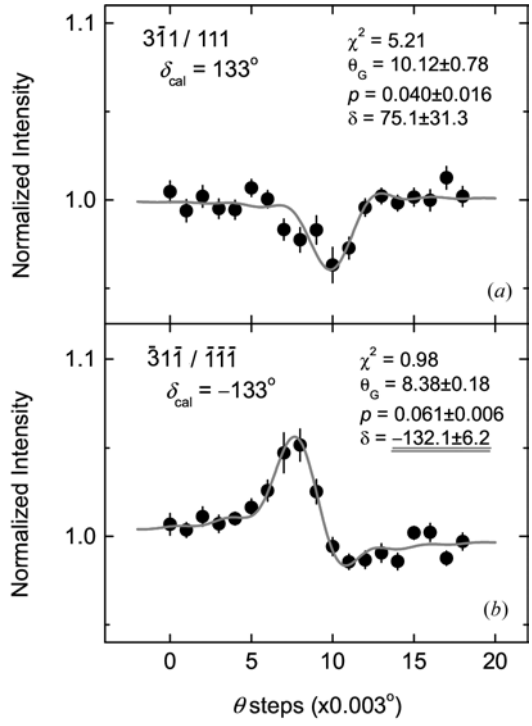

Figure 5
Experimentally measured reference-beam interference profiles of the inverse-beam pair (*a*) **H**/**G** = $3\bar{1}1/111$ and (*b*) −**H**/−**G** = $\bar{3}1\bar{1}/\bar{1}\bar{1}\bar{1}$ of tetragonal lysozyme. The solid curves are fits to the data using equation (5), resulting in the measured triplet phase δ along with interference amplitude p and center θ_G of **G**-reflection rocking curve. With a *larger-amplitude* selection rule given by Shen & Wang (2003), the correct triplet phase is identified by the underlined value, which corresponds to the case with a larger interference amplitude p.

which is very close to the calculated value $\delta_{cal} = 133^\circ$. This example illustrates the improvement in phase accuracy through symmetry-related measurements.

5. Conclusions

In summary, we have shown that, in analogy to standard oscillation data collection, a complete 360° rotation in reference-beam diffraction geometry provides four equivalent measurements of the same triplet phase δ_H for any given primary reflection **H** with **G** as the reference reflection. Two of these cases correspond to reciprocal node **H** passing through the Ewald sphere in 'in' and 'out' conditions, and the other two correspond to inverse coupling reflection **G**−**H** passing through the Ewald sphere in the same fashion. While those for 'in/out' conditions are identical to each other, the interference profiles for **H** and **G**−**H** can be very different and one of them may be more enhanced than the other owing to the structure-factor strengths of the involved reflections.

In addition to the four redundant measurements of δ_H for **H**/**G**/**H**−**G**, symmetric observations through complete triplet inversion with −**G** as the reference reflection provide four additional equivalent ways of measuring triplet phase $-\delta_H$ on the −**H**/−**G**/**G**−**H** and the **H**−**G**/−**G**/**H** interference profiles. These inversion-symmetry-related observations increase the measurement accuracy of the triplet phases in cases where a significant phase-independent intensity contribution exists in a mosaic crystal.

All these additional symmetry observations are supplementary to the existing symmetry elements given by the space group of the crystal structure. Through redundant and symmetry-related measurements, we believe that measured triplet phase errors can be substantially reduced in reference-beam diffraction experiments.

This work is supported by the US National Science Foundation under Grant DMR 97–13424 through CHESS and by National Institute of Health Grant GM-46733 through the Hauptman–Woodward Medical Research Institute in Buffalo, New York.

References

Chang, S. L. (1982). *Acta Cryst.* A**38**, 516–521.
Chang, S. L., Chao, C. H., Huang, Y. S., Jean, Y. C., Sheu, H. S., Liang, F. J., Chien, H. C., Chen, C. K. & Yuan, H. S. (1999). *Acta Cryst.* A**55**, 933–938.
Chang, S. L., King, H. E., Huang, M. T. & Gao, Y. (1991). *Phys. Rev. Lett.* **67**, 3113–3116.
Colella, R. (1974). *Acta Cryst.* A**30**, 413–423.
Mo, F., Mathiesen, R. H., Alzari, P. M., Lescar, J. & Rasmussen, B. (2002). *Acta Cryst.* D**58**, 1780–1786.
Pringle, D. & Shen, Q. (2003). *J. Appl. Cryst.* **36**, 29–33.
Shen, Q. (1986). *Acta Cryst.* A**42**, 525–533.
Shen, Q. (1998). *Phys. Rev. Lett.* **80**, 3268–3271.
Shen, Q. (1999*a*). *Phys. Rev. B*, **59**, 11109–11112.
Shen, Q. (1999*b*). *Phys. Rev. Lett.* **83**, 4784–4787.
Shen, Q. (2000). *Phys. Rev. B*, **61**, 8593–8597.
Shen, Q. & Huang, X. R. (2001). *Phys. Rev. B*, **63**, 174102.
Shen, Q., Kycia, S. & Dobrianov, I. (2000*a*). *Acta Cryst.* A**56**, 264–267.
Shen, Q., Kycia, S. & Dobrianov, I. (2000*b*). *Acta Cryst.* A**56**, 268–279.
Shen, Q., Pringle, D., Szebenyi, M. & Wang, J. (2002). *Rev. Sci. Instrum.* **73**, 1646–1648.
Shen, Q. & Wang, J. (2003). *Acta Cryst.* D**59**, 809–814.
Vaney, M. C., Maignan, S., Riès-Kautt, M. & Ducruix, A. (1995). Deposited with Protein Data Bank, PDB ID = 193L.
Vaney, M. C., Maignan, S., Riès-Kautt, M. & Ducruix, A. (1996). *Acta Cryst.* D**52**, 505–517.
Weckert, E., Holzer, K. Schroer, K., Zellner, J. & Hümmer, K. (1999). *Acta Cryst.* D**55**, 1320–1328.
Weckert, E. & Hümmer, K. (1997). *Acta Cryst.* A**53**, 108–143.
Weckert, E., Schwegle, W. & Hümmer, K. (1993). *Proc. R. Soc. London Ser. A*, **442**, 33–46.